Absolute and convective instabilities in double-diffusive two-fluid flow in a slippery channel

Sukhendu Ghosh, R.Usha[1] and Kirti Chandra Sahu[†]

Department of Mathematics, Indian Institute of Technology Madras, Chennai 600036, India

[†]*Department of Chemical Engineering, Indian Institute of Technology Hyderabad, Yeddumailaram 502 205, Telangana, India*

Abstract

Spatio-temporal instability of miscible two-fluid symmetric flow in a horizontal slippery channel is considered. Both fluids have the same density but different viscosity. A smooth viscosity stratification is created by a thin mixed layer between the fluids due to the presence of two species/scalars, which are diffusing at different rates. **The study finds the existence of a rapidly growing absolutely unstable mode for the configuration with a highly viscous fluid close to the slippery wall and the viscosity difference between the two fluids is large enough.** This instability is less stronger in the case of the equivalent single component two-fluid flow. The viscosity stratified single component (SC) and double-diffusive (DD) slippery flows are absolutely unstable for a wide range of parameter values, when a highly viscous fluid is adjacent to the slippery wall and the mixed layer is close to the channel wall with slip. The instability can be either enhanced or suppressed by wall slip and this is dependent on the location of mixed layer, inertial effects, diffusivity and the log-mobility ratios of the faster and slower diffusing species. This suggests that one can achieve early transition to turbulence due to the absolute instability in a viscosity strat-

[1]Author to whom correspondence should be addressed. Email: ushar@iitm.ac.in

ified channel flow by making the channel walls hydrophobic/rough/porous with small permeability, which can be modelled by the Navier-slip condition.

Keywords: Laminar flow, Mixing, Stability, Fluid mechanics, Hydrodynamics, Multiphase flow

1. Introduction

The linear stability characteristics of a double-diffusive two-fluid three-layer channel flow (the equivalent core-annular configuration in the case of a pipe) with velocity slip at the walls of the channel have been recently investigated by Ghosh *et al.* [1]. The flow system has two miscible fluids with two species having different diffusivity coefficients. The inhomogeneities in solute concentration have been accounted for in terms of viscosity stratification [2–5]. In the presence of double-diffusive (DD) effects, the flow becomes unstable at low Reynolds numbers for a wide range of wave numbers, when the less viscous fluid is adjacent to the slippery channel wall. This is in striking contrast to the stabilization of the flow that is observed for configurations where the viscosity stratification is due to the presence of a single species or scalar [6] (referred as single-component (SC) system). Further, at Reynolds numbers smaller than the critical Reynolds number for the classical Tollmien-Schlichting (TS) mode, a new unstable mode (namely DD mode) has been shown to exist, as the mixed layer of fluids moves towards the channel wall. The DD mode is dominant when the mixed layer overlaps with the critical layer **(the location where the phase speed of the disturbance equals the mean velocity)**. Depending on the flow parameters, the velocity slip at the channel wall has stabilizing or destabilizing influence on the DD flow system. This demonstrate an effective way to control three-layer miscible two-fluid flow in a slippery channel with viscosity stratification.

If disturbances grow locally as well as spread both upstream and downstream directions, the flow is considered to be an absolutely unstable flow. In this case, eventually the entire flow regime becomes unstable and the system

behaves as a self-sustained resonator, oscillating at an intrinsic frequency. In contrast, disturbances amplify as they advect downstream, away from their initial location in a convectively unstable flow [15, 16]. The instabilities observed at relatively low Reynolds numbers in Ghosh *et al.* [1] for a miscible two-fluid flow system with viscosity decreasing towards the walls are convective in nature. However, the configuration with the highly viscous fluid adjacent to the slippery channel walls is unstable due to total viscosity stratification, and in this case velocity slip at the wall destabilizes the DD system (see Ghosh *et al* [1]).

This suggests that if one performs a generalized linear stability analysis in which both the temporal frequency and the spatial wave number are complex, then, it may be possible to clearly predict the boundaries that separate the convectively and absolutely unstable flows in the space of governing dimensionless parameters, such as the Reynolds number, the Schmidt number, the viscosity ratio and the location of mixed layer. In addition, knowledge of boundaries of absolutely unstable regions at relatively low Reynolds numbers, may also provide information on the parameter regimes where mixing of species can be enhanced and this may be useful in relevant applications.

It is important to understand at this stage, the corresponding results that are available for different flow configurations, which are relevant to the present study. In the case of two-dimensional Poiseuille flow of single fluid in a rigid channel, there is no absolute instability for any Reynolds number (Re). The flow is convectively unstable for $Re > Re_{cr}$, where Re_{cr} is the critical Reynolds number (3848.16 based on average flow rate and half channel width). These conclusions on the stability characteristics by Deissler[7] have been based on the numerical solution of Orr-Sommerfeld system for complex frequency and complex wave number for a wide range of Reynolds numbers (Re) and on the asymptotic analysis for large Re. Valette *et al.* [8] have explained the occurrence of defects at die exit, by performing a convective linear stability analysis of a two-layer coextrusion flow for molten polymers.

Their analysis shows that there exists a dominant mode for which the spatial amplification rate reaches its maximum.

Linear stability analysis of miscible two-fluid channel flows reveals that such flows are unstable at low Reynolds numbers and high Schmidt numbers[9, 10]. The investigation by Ern *et al.*[11] for the case of continuous but rapidly varying viscosity stratification in a channel reveals the destabilizing effect of diffusion. The analysis by Sahu *et al.* [12] on the convective and absolute instabilities of miscible two-fluid flow in a channel with uniform layers of highly viscous fluid adjacent to the wall and less viscous fluid in the channel core showed that the bandwidth of parameters for which the flow is absolutely unstable is increased as the diffusivity of the solute in the solvent decreases (i.e. the Schmidt number, Sc increases). Also, the onset of instability is at very low Re and the flow becomes increasingly unstable as Sc increases. In the above study, the viscosity stratification arises due to a pure solvent (say fluid-1) and a solution containing solute/scalar at a particular concentration (say fluid-2), which is a single component flow (SC) system.

The results for a double-diffusive case (DD), where the viscosity stratification arises due to the presence of two solutes/scalars with different diffusivities have also been examined by Sahu and Govindarajon[14]. The instability sets in at very low Reynolds number for a configuration with fluid viscosity decreasing towards the wall. These instabilities are convective in nature. Sahu and Govindarajon[15] examined the spatio-temporal linear stability of a DD miscible two-fluid flow in a rigid channel when the viscosity increases towards the wall. The DD flow is both convectively and absolutely unstable and the growth rates are higher as compared to the corresponding SC system. Further, the regime of instability is increased in the presence of a second solute/scalar that decreases the average Schmidt number. This is in contrast to the instability that sets in at very low Reynolds number in the SC flow and which becomes unstable as the diffusivity of the solute in the solvent decreases (i.e. as the Schmidt number increases)[12]. Also the band-

width of parameters for which the DD flow is unstable is much wider than that for SC flow. The recent review article by Govindarajan and Sahu [16] extensively discussed instabilities in viscosity stratified flows.

It is of interest, therefore, to examine whether the parameter regimes of convective and absolute instabilities predicated for DD [15] as well as SC [12] flow systems in a rigid channel are influenced by the velocity slip at the channel walls. Such efforts in understanding the effects of slip at the wall in laminar channel flows gain importance due to their occurrence in many applications such as lubrication, high-speed rarefied flows [17, 18], drag reduction in microchannel flows[19–21], polymer melt[22], technological and biological drag reduction surfaces[23, 24] and microfludics[25, 26], where the velocity of viscous fluid exhibits a tangential slip at the wall. The possibility of slip at the solid boundary has been confirmed by experimental predictions[22, 25] and molecular dynamic simulations[26]. In fact, the slip effects on the stability characteristics of a Poiseuille flow in a channel for a single fluid[27–32] and for viscosity-stratified immiscible fluids[33, 34] have been reported and these investigations can be thought of describing the results for flow systems in channels with porous/rough/hydrophobic walls, which can be modelled by velocity slip at the surfaces[19, 20, 35, 36, 38]. **In addition, the slip condition can also be modeled by eddies over wavy/rough surfaces [39–42].**

The present study extends the investigation of Sahu and Govindarajan [15] on the absolute and convective instabilities of double-diffusive miscible two-fluid flow in a rigid channel to that in a slippery channel and examines the effects of wall slip through a linear stability analysis. The analysis investigates a configuration with viscosity increasing towards the slippery channel wall. For example, if a PDMS (polydimethylsiloxane) channel is hosting a two-fluid flow of cold water and hot glycerol solution (where $R_s > 0$, $R_f < 0$; R_s, R_f are log-mobility ratios of the slower and faster diffusing scalars, namely temperature and glycerol, defined

later in section II), then the present study addresses the spatio-temporal linear stability analysis of a DD flow system with a configuration where highly viscous fluid is near the wall (which implies $R_f + R_s > 0$). A temporal linear stability analysis by Ghosh *et al.*[1] shows that there is a large unstable region for a wide range of wave numbers due to total viscosity stratification. The present study attempts (i) to find the boundaries of convectively and absolutely unstable regions for this configuration under wall slip, and (ii) to answer the questions: are there parameter regimes where the DD system in a rigid channel is not absolutely or convectively unstable but it is so in a slippery channel and vice versa.

The analysis is also extended to the SC system. For example one can consider a PDMS (polydimethylsiloxane) channel hosting an miscible oil-water flow and perform a stability analysis for a configuration in which oil (highly viscous fluid) flows adjacent to the hydrophobic wall. For this configuration it has been shown in Ghosh *et al.*[6] that the flow system is highly unstable. In this case, surface energy will be high, the contact angle will be small (less than 90°) and the slip effect is not sufficient to reduce the shear at the wall. This results in the flow system to become more unstable.

The paper is organized as follows: the mathematical formulation and base state are presented in section II. The results are discussed in section III, and the conclusions are given in section IV.

2. Mathematical Formulation

2.1. Governing equations

A spatio-temporal linear stability analysis of a two-dimensional Poiseuille flow of miscible Newtonian and incompressible fluids having the same density and different viscosities in a slippery channel of **height** $2H$ is considered (see Fig. 1). Both the fluids contain the same solvent, but have two species (S and F) diffusing at different rates; S and F represent the slower and faster diffusing species, respectively. $\mathcal{D}_f$ and $\mathcal{D}_s$ are the diffusion rates of

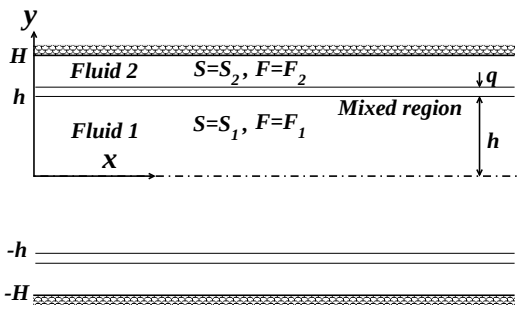

Figure 1: Schematic of the flow system considered. The core and annular regions of the slippery channel contain fluids '1' and '2', respectively. Here fluid '1' occupies the region $-h \leq y \leq h$ and both the fluids are separated by a mixed layer of uniform thickness q. The slippery walls of the channel are located at $y = \pm H$.

F and S with their ratio $\delta = \frac{\mathcal{D}_f}{\mathcal{D}_s} > 1$. A mixed layer of thickness q separates fluid-1 (occupying the core of the channel) and fluid-2 (present near the slippery walls of the channel) containing species/scalars S, F of concentration S_1, F_1, with net viscosity μ_1 and S_2, F_2, with net viscosity μ_2 respectively. **In this investigation, the thickness of the mixed layer (q) is considered as a constant. Generally, the thickness of the mixed layer should depend upon the concentration profiles of the species and so it is a function of x. The present study is based on the parallel flow assumption in the mixed layer. The parallel flow approximation is valid at large Reynolds and Peclet numbers, and we restrict ourselves to presenting results in this regime. One can easily show that this mixed layer diffuses at a rate proportional to the inverse of Peclet number ($Pe = Re\,Sc$). Thus, the downstream growth of the mixed layer is small at high Reynolds number. So, for Reynolds number of the order of 100, the parallel flow approximation is justified unless $Sc << 1$. As our Reynolds numbers considered are always greater than 100, the assumption of constant q is valid (see Appendix-A).** The flow dynamics is analyzed using the cartesian co-ordinate system (x, y), where x and y represent the stream-wise and wall-normal directions, respectively. The slippery walls are

at $y = \pm H$. In view of symmetry of the flow system about the centreline $y = 0$, the problem is formulated in $0 \leq y \leq H$. The mixed layer of thickness q is located at $h \leq y \leq h + q$ (see Fig. 1).

In reality, the mixing process for F is quicker than that for S, as F is diffusing faster than the S. Which implies one can get two mixed layers of different thickness q_f (for F) and q_s (for S) with $q_f < q_s$. As the Reynolds numbers considered in the present work are large, the Péclet numbers ($ScRe$ and $ScRe/\delta$) for the faster and slower diffusing species are also very large for $Sc > 1$. In view of the above, we neglect the difference between the mixed layer thicknesses of the slower and faster diffusing species. It is noted that the aforementioned approximation may not be valid for $Sc << 1$. One can obtain exact values of q_f and q_s from direct numerical simulation or experiment.

In the present study, we want to examine the wall slip effects on the absolute and convective instabilities of DD system by taking the mixed layer between the two fluids in such a way that the base viscosity variation within the mixed layer of small thickness is very smooth, continuous and monotonic. Therefore, in this study, the computations are performed by considering $q_f = q_s = q$.

The viscosity of the two fluids is assumed to depend exponentially on concentration of the solute species and is taken as[14]:

$$\mu = \mu_1 \exp\left[R_s\left(\frac{S - S_1}{S_2 - S_1}\right) + R_f\left(\frac{F - F_1}{F_2 - F_1}\right)\right], \tag{1}$$

where $R_s = (S_2 - S_1)\dfrac{\partial}{\partial S}(\ln \mu)$, $R_f = (F_2 - F_1)\dfrac{\partial}{\partial F}(\ln \mu)$ are the log-mobility ratios of the scalars S and F respectively. **In Eq. (1), $\mu(y)$ represents the piecewise viscosity profile (dimensional) for all the liquid layers depending on the values of the general concentration function S, F in different layers. μ_1 is the viscosity of the fluid layer-1. Therefore**

the viscosity function $\mu(y)$ is given as a function of concentration of the species and μ_1(which will help us in non dimensionalization process). We see from (1) that the basic viscosity is given by

$$\mu = \begin{cases} \mu_1 & \text{if } 0 \le y \le h, \\ \mu_m(y) & \text{if } h \le y \le h+q, \\ \mu_2 & \text{if } h+q \le y \le H, \end{cases} \tag{2}$$

where $\mu_2 = \mu_1 \exp(R_s + R_f)$ and $\mu_m(y) = \mu_1 \exp\left[R_s\left(\frac{S-S_1}{S_2-S_1}\right) + R_f\left(\frac{F-F_1}{F_2-F_1}\right)\right]$. Here, $\mu_m(y)$ gives the viscosity distribution in the mixed layer. **Note that, in fluid layer-1, $S = S_1, F = F_1$ therefore $\mu(y) = \mu_1$ and in fluid layer-2, $S = S_2, F = F_2$ hence $\mu(y) = \mu_2$.**

The flow dynamics is governed by the continuity, the Navier-Stokes and the convection-diffusion equations for the two solute species. The boundary conditions at the centerline and at the slippery upper wall of the channel are

$$\frac{\partial u}{\partial y} = 0, \quad v = 0 \quad \text{at } y = 0, \tag{3}$$

$$u = -\beta_1 \frac{\partial u}{\partial y}, \quad v = 0 \quad \text{at } y = H, \tag{4}$$

where β_1 is the dimensional slip parameter, u and v are the velocity components in the x and y directions, respectively. The dimensionless governing equations and the boundary conditions are obtained using the following scaling:

$$x^* = \frac{x}{H},\ y^* = \frac{y}{H},\ t^* = \frac{Q}{H^2}t,\ (u^*, v^*) = \frac{H}{Q}(u, v),\ p^* = \frac{H^2}{\rho Q^2}p,\ \mu^* = \frac{\mu}{\mu_1},\ h^* = \frac{h}{H},$$
$$q^* = \frac{q}{H},\ m = \frac{\mu_2}{\mu_1},\ \beta = \frac{\beta_1}{H},\ s^* = \frac{S - S_1}{S_2 - S_1},\ f^* = \frac{F - F_1}{F_2 - F_1},\ \mu_m^* = \frac{\mu_m(y)}{\mu_1}, \tag{5}$$

where Q is the flow rate per unit distance in the spanwise direction, p is the pressure and t is the time. The dimensionless governing equations and boundary conditions (after suppressing $*$) are

$$u_x + v_y = 0, \tag{6}$$

$$u_t + uu_x + vu_y = \frac{\partial}{\partial x}\left[-p + \frac{2}{Re}\mu u_x\right] + \frac{\partial}{\partial y}\left[\frac{1}{Re}\mu(u_y + v_x)\right], \tag{7}$$

$$v_t + uv_x + vv_y = \frac{\partial}{\partial x}\left[\frac{1}{Re}\mu(u_y + v_x)\right] + \frac{\partial}{\partial y}\left[-p + \frac{2}{Re}\mu v_y\right], \tag{8}$$

$$s_t + us_x + vs_y = \frac{1}{Pe}[s_{xx} + s_{yy}], \tag{9}$$

$$f_t + uf_x + vf_y = \frac{\delta}{Pe}[f_{xx} + f_{yy}], \tag{10}$$

where $\mu = \exp[R_s s + R_f f]$, such that the values of s, f are 0 and 1 for fluids '1' and '2', respectively. The boundary conditions are

$$u_y = 0, \quad v = 0 \quad \text{at} \quad y = 0, \tag{11}$$

$$u = -\beta u_y, \quad v = 0 \quad \text{at} \quad y = 1. \tag{12}$$

The above system is governed by the Reynolds number $Re = \rho Q/\mu_1$, the Péclet number $Pe = Q/\mathcal{D}_s$, the ratio of the diffusion coefficients of the species, $\delta = \mathcal{D}_f/\mathcal{D}_s$, the Schmidt number $Sc = Pe/Re$ and the dimensionless slip parameter $\beta = \beta_1/H$. For the faster diffusing fluid, the effective Schmidt number is Sc/δ.

Note that, the concentration profiles of the slower and faster diffusing species are dependent upon x. But in the discussion presented in Appendix-A, we have shown that for high Peclet number the downstream variation of f, s (in dimensional form F, S) are very small, which implies that the variations of F, S are very small with respect to x in any small interval $x \in [x_0, x_1]$. Also, S_1, F_1, S_2, F_2 are the values of concentration at initial stage (time $t = 0$), so we took all these as constants. However, for the later time the concentration profiles satisfy Eq. (9) and (10).

The base state and the modified linear stability equations derived using normal mode analysis are similar to those presented in Ghosh *et al.*[1] but are again given here for completeness.

2.2. Base state

The base state is obtained by solving the equations (6)−(10) along with the boundary conditions (11)−(12) by assuming steady state and locally parallel flow:

$$Re\left(\frac{dP_B}{dx}\right) = \frac{d}{dy}\left[\mu_B(y)\frac{dU_B(y)}{dy}\right]. \tag{13}$$

The solution of the above equation is given by

$$U_B(y) = \begin{cases} \dfrac{G}{2}\left[y^2 - h^2 + \dfrac{(h+q)^2 - 1 - 2\beta}{m} - 2\int\limits_h^{h+q} \dfrac{y}{\mu_m(y)}\,dy\right] & \text{if } 0 \le y \le h, \\ \dfrac{G}{2}\left[\dfrac{(h+q)^2 - 1 - 2\beta}{m} - 2\int\limits_y^{h+q} \dfrac{y}{\mu_m(y)}\,dy\right] & \text{if } h \le y \le h+q, \\ \dfrac{G}{2m}(y^2 - 1 - 2\beta) & \text{if } h+q \le y \le 1, \end{cases} \tag{14}$$

where $G = RePB_x$ and

$$\mu_B(y) = \begin{cases} 1 & \text{if } 0 \le y \le h, \\ \mu_m(y) = \exp\left[R_s\, s_B(y) + R_f\, f_B(y)\right] & \text{if } h \le y \le h+q, \\ m = \exp(R_s + R_f) & \text{if } h+q \le y \le 1. \end{cases} \tag{15}$$

Here, the subscript B designates the base state variables and s_B and f_B are taken as fifth degree polynomials in y in the mixed layer [14], such that the concentration profile is smooth up to the second derivative at $y = h$ and $y = h + q$:

$$f_B(y) = s_B(y) = \begin{cases} 0 & \text{if } 0 \le y \le h, \\ \sum\limits_{i=1}^{6} a_i y^{i-1} & \text{if } h \le y \le h+q, \\ 1 & \text{if } h+q \le y \le 1, \end{cases} \tag{16}$$

where a_i, $i = 1, 2, \ldots, 6$ are given by

$$a_1 = -\frac{h^3}{q^5}(6h^2 + 15hq + 10q^2), \quad a_2 = \frac{30h^2}{q^5}(h+q)^2,$$
$$a_3 = -\frac{30h}{q^5}(h+q)\,(2h+q), \quad a_4 = \frac{10}{q^5}(6h^2 + 6hq + q^2), \tag{17}$$
$$a_5 = -\frac{15}{q^5}(2h+q), \quad a_6 = \frac{6}{q^5}.$$

The concentration profiles defined in equation (16) can only be found at x location shorter than the solutal entry length. This implies that the analysis takes place at a point of the channel where the thickness of the mixed layer q is expected to grow up when increasing x. Therefore, the analysis that follows is based on a kind of "Frozen Time" approximation[1]. Here, $f_B(y), s_B(y)$ are taken as the base or initial solution for the concentration profiles which are not derived from equations (9) and (10). These are the solution at time $t = 0$ and at the position where the mixing of two fluids of different viscosity (separated by a plate as mentioned in Appendix-A) just starts. In the later time s, f are the solutions of Eqs. (20) and (21) (see in the next section). Naturally, this new solutions are different from $f_B(y), s_B(y)$ and dependent on the diffusivity of the two solutes/species. That's why we mention the above statement in our analysis. Also, we want to check the stability of the system after perturbation of the above initial solution so we can do the analysis at any distance with time change. It is known from the Appendix-A that the steady mean concentration c (say) at any location satisfies the equation,

$$U\frac{\partial c}{\partial x} + V\frac{\partial c}{\partial y} = \frac{1}{Pe}\left[\frac{\partial^2 c}{\partial x^2} + \frac{\partial^2 c}{\partial y^2}\right].$$

Using the boundary layer approximations $V \ll U$ and $\frac{\partial^2}{\partial x^2} \ll \frac{\partial^2}{\partial y^2}$, we can get $U\frac{\partial c}{\partial x} \simeq \frac{1}{Pe}\left(\frac{\partial^2 c}{\partial y^2}\right)$. Which implies the scaling $U\frac{c}{x} \simeq \frac{1}{Pe}\left(\frac{c}{q^2}\right)$

or, $q \simeq \sqrt{x/(U\,Pe)}$ **(where** $Pe = Sc\,Re$**). Now for a fixed value of** $q = 0.1$ **with** $h = 0.6$ **(chosen for most of the computations) and base velocity** $U \approx 0.6$ **(the exact value depends on the viscosity ratio** m**) one can found** $x \approx 60$**, when** $Re = 200$ **and** $Sc = 50$**. That means in an experiment with a channel hight** $2H = 1cm$ **our analysis is valid at a stream wise distance** $30cm$ **(as** $H = 0.5$ **is the length scale).**

The dimensionless pressure-gradient is determined by requiring that $\int_0^1 U_B(y)dy = 1$. It is to be noted that the component having negative (positive) log-mobility ratio makes the viscosity decrease (increase) towards the slippery wall and hence stabilizing (destabilizing).

2.3. Linear stability analysis

The spatio-temporal linear stability of the base flow (equations (14)−(17)) is investigated using normal mode analysis. The absolute growth rates are obtained using Brigg's-type method[43, 44]. The flow variables are taken as

$$(u, v, p, s, f) = (U_B(y), 0, P_B(x), s_B(y), f_B(y)) + (\hat{u}, \hat{v}, \hat{p}, \hat{s}, \hat{f})(y)\exp\left[\mathrm{i}\left(\alpha x - \omega t\right)\right], \tag{18}$$

where $\mathrm{i} \equiv \sqrt{-1}$, α and $\omega = \alpha c$ are the wave number and the frequency of the infinitesimal two-dimensional disturbance (designated by a hat). Here c is the complex phase speed. Both α and ω are complex numbers. The temporal growth or decay of the disturbance is given by the imaginary part of ω (say, ω_i) when wave number α is real. The perturbation viscosity $\hat{\mu}$ is given by $\hat{\mu} = (\frac{\partial \mu_B}{\partial s_B}\hat{s} + \frac{\partial \mu_B}{\partial f_B}\hat{f})$. The velocity perturbations are expressed in terms of the stream function perturbation $\phi(= \hat{\phi}\exp(\mathrm{i}\left(\alpha x - \omega t\right)))$ such that $(\hat{u}, \hat{v}) = (\phi_y\,, -\phi_x)$. Modified Orr-Sommerfeld system is then derived from the dimensionless governing equations and the boundary conditions (6)−(12) using the standard procedure (see e.g. Drazin & Reid [45]) and are given by

(after suppressing hat (ˆ) symbols)

$$\mathrm{i}\alpha\, Re\left[\phi''(U_B-c)-\alpha^2\phi(U_B-c)-U_B{}''\phi\right]=\mu_B\phi''''+2\mu_B{}'\phi'''+(\mu_B{}''-2\alpha^2\mu_B)\phi''$$
$$-2\alpha^2\mu_B{}'\phi'+(\alpha^2\mu_B{}''+\alpha^4\mu_B)\phi+U_B{}'\mu''+2U_B{}''\mu'+(U_B{}'''+\alpha^2U_B{}')\mu, \quad (19)$$

$$\mathrm{i}\alpha\, Pe\left[(U_B-c)s-s_B{}'\phi\right]=(s''-\alpha^2 s), \quad (20)$$

$$\mathrm{i}\alpha\, Pe\left[(U_B-c)f-f_B{}'\phi\right]=\delta(f''-\alpha^2 f), \quad (21)$$

$$\phi' = -\beta\phi'', \quad \phi=s=f=0 \quad \text{at} \quad y=1, \quad (22)$$

$$\phi' = \phi'''=s'=f'=0 \quad \text{at} \quad y=0, \quad \text{(sinuous mode)}, \quad (23)$$

where prime ($'$) denotes differentiation with respect to y. The above equations contain the terms that arise due to the continuous variations of the base flow velocity and viscosity perturbations. The system of equations (19)−(23) constitute an eigenvalue problem and determine the linear stability characteristics of infinitesimal two-dimensional disturbance in double-diffusive miscible three-layer pressure-driven flow in a channel with velocity slip at the walls. The classical Orr-Sommerfeld equation [45] can be recovered from the above equation by neglecting the terms due to viscosity stratification. The modified Orr-Sommerfeld system is solved numerically by the public domain software, LAPACK, after discretization of the domain using Chebyshev spectral collocation method (Canuto *et al.*[46]). The results are presented for sinuous mode (described by equation (23) at the centerline of the channel) as it was observed to be the dominant mode for the range of parameters considered. A sufficiently large number of grid points are taken in the mixed layer, since the gradients are large in this layer. This is achieved by using the stretching function (Govindarajan [10])

$$y_j=\frac{a}{\sinh(by_0)}\left[\sinh\{(y_c-y_0)b\}+\sinh(by_0)\right], \quad (24)$$

where y_j are the locations of the grid points, a is the mid point of the mixed layer and y_c is a Chebyshev collocation point, given by

$$y_c=0.5\left\{\cos\left[\pi\frac{(j-1)}{(n-1)}\right]+1\right\}, \quad (25)$$

and

$$y_0 = \frac{1}{2b} \ln \left[\frac{1 + (\mathrm{e}^b - 1)a}{1 + (\mathrm{e}^{-b} - 1)a} \right], \tag{26}$$

where n is the number of collocation points and b is the degree of clustering. In the present study, we performed our computations by taking $b = 8$ and using 121 collocation points. This gives an accuracy of at least five decimal places in the range of parameters considered.

The approach used in the previous investigations to analyze the stability of mixing layers, jets and wakes, single-solute/two-solute miscible two-fluid flows in rigid channels and in plasma flows [12, 13, 43, 44, 47–51] is employed to determine whether the flow is absolutely or convectively unstable (see Appendix-B).

The linearized differential operator represents a dispersion relation, $\omega_i = \omega_i(\alpha, Re, Sc, R_s, R_f, h, q, \beta)$ in complex (ω, α) space. The corresponding Green's function, $G(x, y, t)$, gives the response of the linearized system to an impulse perturbation. For a chosen mode, the long-time behaviour of G along different "rays", along which x/t is constant, is then analyzed[15]. It may be noted that this quantity corresponds to the group velocity of the mode, that is,

$$\frac{x}{t} = \frac{\partial \omega}{\partial \alpha}(\alpha). \tag{27}$$

We now distinguish between the maximum temporal growth rate, $\omega_{i,max}$ corresponding to a real wave number α, and the imaginary part of the "absolute frequency", $\omega_0 = \omega(\alpha_0)$, corresponding to the "absolute wave number" α_0, at which the saddle point condition

$$\frac{\partial \omega}{\partial \alpha}(\alpha_0) = 0 \tag{28}$$

is satisfied. This corresponds to the ray, $x/t = 0$, which has zero group velocity. We have absolute instability if imaginary part of $\omega_0 = \omega_{0i} > 0$; that is, if the absolute growth rate (ω_{0i}) is positive. From Eqs.(27) and (28), it is clear that we then have an impulse response growing locally, and usually

spreading both upstream and downstream from its source. On the other hand, if $\omega_{0i} < 0$ but $\omega_{i,max} > 0$, the impulse disturbances grow as they move downstream from their source, giving rise only to a convectively unstable flow.

3. Results and discussion

We begin the presentation of our results by validating our linear stability solver by computing the range of Reynolds number for which a plane Poiseuille flow in rigid/slippery channel is convectively unstable. Fig. 2 presents the maximum growth rate as a function of Reynolds number. As discussed ablove, the flow is convectively unstable when $\omega_{i,max} > 0$, and the Reynolds number above which this happens is known as critical Reynolds number (Re_{cr}). The result obtained using the present solver for the rigid channel flow ($\beta = 0; Re_{cr} = 3848.16$) agrees exactly with that of Deissler[7] and Drazin & Reed[45] (after using the appropriate velocity and length scales). Further, the critical Reynolds numbers for the convective instability of the flow in slippery/hydrophobic channel ($\beta = 0.01$, $Re_{cr} = 4654.74; \beta = 0.02$, $Re_{cr} = 7184.85$) agree with those obtained by Lauga and Cossu[30].

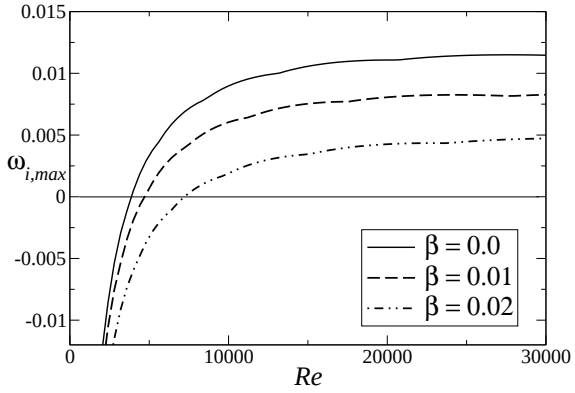

Figure 2: Maximum temporal growth rate ($\omega_{i,max}$) as a function of Reynolds number (Re) for a plane Poiseulle flow in rigid/slippery channel. The result with $\beta = 0$ corresponds to rigid channel flow.

The convective instabilities associated with the DD and the SC systems with the highly viscous fluid adjacent to the slippery walls are first analyzed by taking the wave number α to be real (i.e the real part of α, $\mathbf{Re}(\alpha) = \alpha_r \neq 0$ and the imaginary part of α, $\mathbf{Im}(\alpha) = \alpha_i = 0$). The flow systems have highly viscous fluid adjacent to the slippery wall. The spatio-temporal stability analysis for the DD two-fluid flow in a rigid channel analyzed by Sahu and Govindarajan[15] shows that the DD system with highly viscous fluid adjacent to the walls of the channel is absolutely unstable above a certain R_s value, for a fixed R_f value. A value of $R_s = 5.2$ (when $R_f = -0.5$) at which the above system is absolutely unstable is chosen for comparison. In Fig. 3(a), we plot the growth rate of the most unstable disturbance maximized over all wavelengths ($\omega_{i,max}$) as a function of Reynolds number Re for the DD system with $R_s = 5.2$, $R_f = -0.5$, $Sc = 50$, $\delta = 10$. The temporal growth rate (ω_i) as a function of real wave number α (α_r) is presented in Fig. 3(b) for $Re = 200$, for the above DD system. The results for the equivalent SC(E) system are also shown in Fig. 3(b), when $R_s = 4.7$, $R_f = 0.0$, $Sc = 9.09$, $\delta = 10$. Here, SC(E) designate the equivalent SC system that has the same average diffusivity ($\mathcal{D}_{SCE} = (\mathcal{D}_s + \mathcal{D}_f)/2$) as the DD system, which gives the equivalent Schmidt number of the SC(E) flow as $2Sc/(1+\delta)$ (in this particular case, the value of Sc is $100/11 = 9.09$). The other parameters are fixed as $h = 0.6$ and $q = 0.1$. The solid and dashed curves without symbols (with symbols) correspond to results for the DD system (SC(E) system) for $\beta = 0.0$ and $\beta = 0.1$ respectively. Fig. 3(a) reveals that the DD system in a rigid/slippery channel is unstable at far lower Reynolds numbers than the equivalent SC system (SC(E)). The SC(E) system is more unstable than the DD system at higher Reynolds numbers. The DD (SC(E)) flow in a slippery channel registers a higher $\omega_{i,max}$ at lower (higher) Reynolds numbers indicating the destabilizing role of slip in the two flow systems. The dispersion curves presented for each β in Fig. 3(b) show a finite range of wave numbers over which $\omega_i > 0$, indicating linear instability in the DD systems

in rigid/slippery channel. For the DD system in a slippery channel, higher growth rate and wider range of unstable numbers are observed. The SC(E) system is stable for this set of parameters.

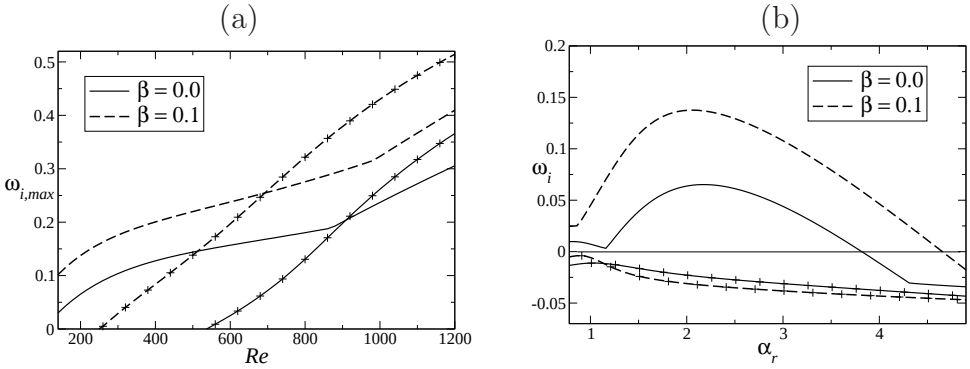

Figure 3: Convective instability for the DD and the SC(E) two-fluid flow in a rigid ($\beta = 0.0$) and a slippery ($\beta = 0.1$) channel. (a) Maximum growth rate ($\omega_{i,max}$) as a function of Reynolds number (Re); (b) temporal growth rate (ω_i) as a function of real wave number α_r for $Re = 200$. The parameters for the DD flow are $R_s = 5.2$, $R_f = -0.5$, $Sc = 50$, $\delta = 10$ and for the SC(E) flow are $R_s = 4.7$, $R_f = 0.0$, $Sc = 9.09$, $\delta = 10$. The other parameters are $h = 0.6, q = 0.1$. The solid and dashed curves without symbols (with symbols) correspond to the results for the DD (SC(E)) system for $\beta = 0.0$ and $\beta = 0.1$ respectively.

The 'cut-off' wave number and the wave number of the 'most-dangerous' mode for the DD system in a slippery channel are smaller than those observed in case of the DD system in a rigid channel. By 'cut-off' and 'most-dangerous' wave number correspond to the values of α beyond which $\omega_i > 0$ and for which ω_i is maximum, respectively.

It is interesting to note that the SC system (having one component only, says S) with $R_s = 3.5$, $\delta = 1$, $Sc = 50$, $Re = 200$, $h = 0.6$ and $q = 0.1$ is convectively unstable with significantly higher growth rate (shown in Fig. 4) as compared to the DD system (shown in Fig. 3(b)). An increase in slip at the wall increases the temporal growth and the range of unstable wave numbers, indicating the destabilizing effects of β.

The isocontours of frequency ω_r (Fig. 5(a) for $\beta = 0.0$; Fig. 5(b) for $\beta = 0.1$) and growth rate ω_i (Fig. 5(c) for $\beta = 0.0$; Fig. 5(d) for $\beta = 0.1$)

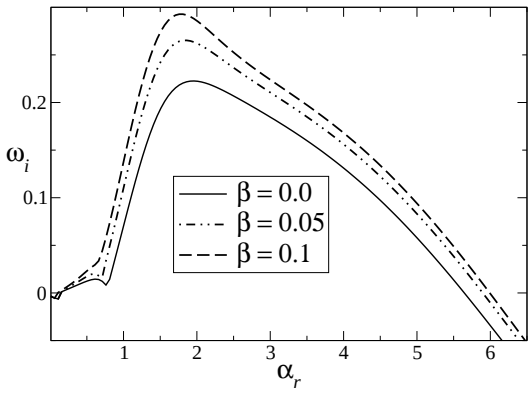

Figure 4: Temporal growth rate (ω_i) as a function of real wave number $\alpha = \alpha_r$ when $Re = 200$ for the SC system. Here $R_s = 3.5$, $Sc = 50$, $\delta = 1$, $h = 0.6$ and $q = 0.1$.

are presented in the complex wave number ($\mathbf{Re}(\alpha)$−$\mathbf{Im}(\alpha)$) plane for a DD system at $Re = 200$. The other parameters are fixed at $R_s = 4.0$, $R_f = -0.5$, $Sc = 50$, $\delta = 10$, $h = 0.6$ and $q = 0.1$. Here, the values of R_f and R_s indicate that the faster diffusing component is stabilizing and the slower diffusing component is destabilizing. Figs. 5(a) and 5(c) correspond to those obtained by Sahu and Govindarajan[15] but are presented here for the sake of comparison. Inspection of these figures reveal that the DD system is absolutely unstable for both $\beta = 0.0$ and $\beta = 0.1$. It can be seen that the absolute growth rate for the slippery channel ($\beta = 0.1, \omega_{0i} = 0.066$) is much higher than that for the rigid channel ($\beta = 0.0, \omega_{0i} = 0.043$). The absolute frequency ω_0 at the saddle point for $\beta = 0.0$ and $\beta = 0.1$ are $1.178 + 0.043$i and $1.304 + 0.066$i, respectively. There is an increase in phase speed as wall slip increases. The equivalent SC(E) system is not absolutely unstable for the above set of parameters values as the temporal growth rate is negative for all wave numbers (figure not presented here) and it is well known[43] that the maximum temporal growth rate ($\omega_{i,max}$) is an upper bound for the absolute growth rate (ω_{0i}).

The usual SC system in a rigid channel with $R_s = 3.5$, $\delta = 1$, $Sc = 50$, $Re = 200$, $h = 0.6$ and $q = 0.1$ (Fig. 6(a) for $\beta = 0.0$) has absolute

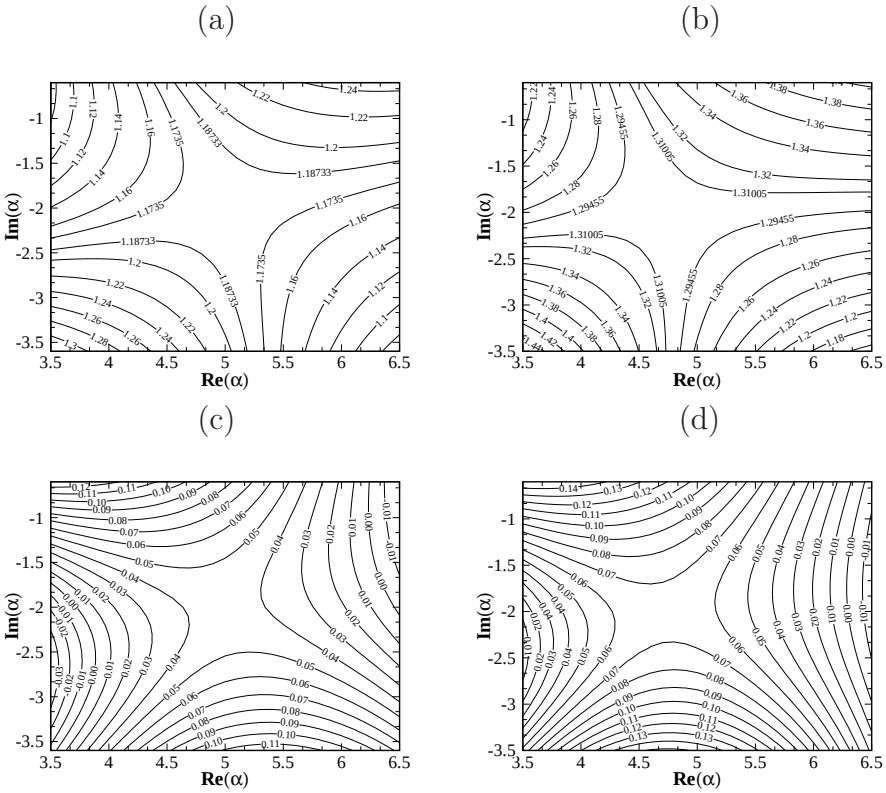

Figure 5: The isocontours of ω_r and ω_i in the complex wave number plane for the DD system. Here $R_s = 4.0$, $R_f = -0.5$, $Sc = 50$, $\delta = 10$, $h = 0.6$ and $q = 0.1$. (a) and (b) represent ω_r contours for $\beta = 0.0$ and 0.1. (c) and (d) represent ω_i contours for $\beta = 0.0$ and 0.1.

frequency $\omega_0 = 1.175 - 0.001\text{i}$ at the saddle point and is damped out rapidly (as $\omega_{0i} = -0.001 < 0$); and therefore flow is not absolutely unstable for this set of parameter values. But this SC system is convectively unstable as is evident from Fig. 4, for $\beta = 0.0$ ($\omega_{i,max} > 0$). It is to interesting to see that the above SC system in a slippery channel (Fig. 6(b) for $\beta = 0.1$) is absolutely unstable with $\omega_{0i} = 0.026 > 0$ ($\omega_0 = 1.301 + 0.026\text{i}$) at the saddle point. Therefore, the slippery channel SC flow for this set of parameters is convectively (as is evident from Fig. 4, $\beta = 0.1$) as well as absolutely unstable.

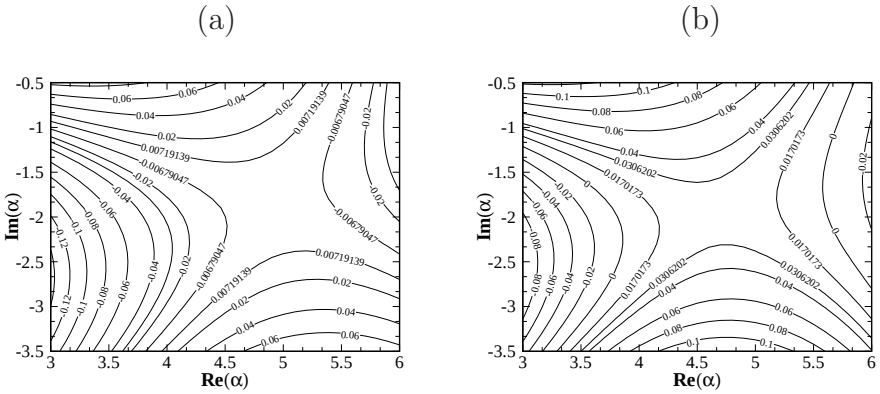

Figure 6: The isocontours of ω_i in the complex wave number plane for the SC system. Here, $R_s = 3.5$, $\delta = 1$, $Sc = 50$, $h = 0.6$ and $q = 0.1$. (a) for $\beta = 0.0$ and (b) for $\beta = 0.1$.

It is worth observing that both the DD flow and the SC flow in a slippery channel exhibit a trend, namely, destabilizing the flow system, that is dictated by the slower diffusing species. The DD flow in a slippery channel shows higher absolute instability than the SC flow although the SC flow has higher average diffusivity rate and average viscosity stratification than the DD flow.

It is interesting to analyze the DD flow for the case $R_f + R_s > 0$, but with slower diffusing component stabilizing ($R_s < 0$) and the faster diffusing component destabilizing ($R_f > 0$). Fig. 7 shows the results for the DD flow (ω_i as a function of $\alpha = \alpha_r$ for $Re = 200$, $R_s = -0.5$, $R_f = 4.0$, $Sc = 50$, $\delta = 10$, $h = 0.6$ and $q = 0.1$) in a rigid ($\beta = 0.0$, solid curves with no symbols) and slippery ($\beta = 0.1$, dashed curves with no symbols) channel. For the DD flow system, ω_i is higher in the case of slippery channel than in the case of rigid channel; also, the range of unstable wave numbers α_r is wider for $\beta = 0.1$. The results for corresponding equivalent SC(E) flow for $Sc = 9.09$, $\delta = 10$, $R_s = 3.5$, $R_f = 0$, $h = 0.6$ and $q = 0.1$ (solid and dashed curves with symbols for $\beta = 0.0$ and $\beta = 0.1$ respectively) reveal that the equivalent SC(E) flow is more convectively unstable than the DD flow in the rigid as well as slippery channel.

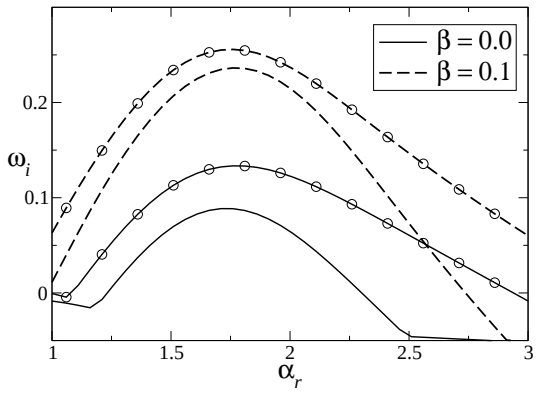

Figure 7: Convective instability of the DD and the SC(E) flows in a rigid ($\beta = 0.0$) and a slippery ($\beta = 0.1$) channel, when $Re = 200$. The temporal growth rates (ω_i) are displayed for the DD flow (curves without symbols; $R_s = -0.5$, $R_f = 4.0$, $Sc = 50$, $\delta = 10$, $h = 0.6$ and $q = 0.1$) and for the SC(E) flow (curves with symbols; $R_s = 3.5$, $R_f = 0$, $Sc = 9.09$, $\delta = 10$, $h = 0.6$ and $q = 0.1$). Here, the slower diffusing species (S) has stabilizing effect.

The DD flow case where the slower diffusing component is destabilizing ($R_s > 0$) and faster diffusing component is stabilizing ($R_f < 0$) with $R_f + R_s > 0$ is revisited again and the role of wall slip on the absolute growth rate as a function of R_s is assessed for different mixed layer thickness ($q = 0.1$, Fig. 8(a); $q = 0.05$, Fig. 8(b)). The other parameters are fixed at $Re = 200$, $R_f = -0.5$, $Sc = 50$, $h = 0.6$ and $\delta = 10$. When the mixed layer is thicker ($q = 0.1$, Fig. 8(a)), the absolute growth rate ω_{0i} is significant for a DD flow in a slippery channel ($\beta = 0.05$) than in a rigid channel ($\beta = 0.0$) for small values of R_s; but when $q = 0.05$ (Fig. 8(b)), for these values of R_s, the DD flow in a rigid channel has significant absolute growth as compared to that in a slippery channel. ω_{0i} is nonmonotonic as a function of slip parameter β for smaller R_s values, when mixed layer is thicker ($q = 0.1$). At higher values of R_s, slip exhibits a destabilizing role by increasing the absolute growth rate and qualitative behaviour is not affected by the thickness of the mixed layer. Further, ω_{0i} is more significant for a thinner mixed layer (Fig. 8(b)). Therefore, a decrease in mixed layer thickness q destabilizes the DD flow system absolutely by increasing the absolute growth rate (ω_{0i}) and the result

is consistent with the linear stability results of the DD flow.

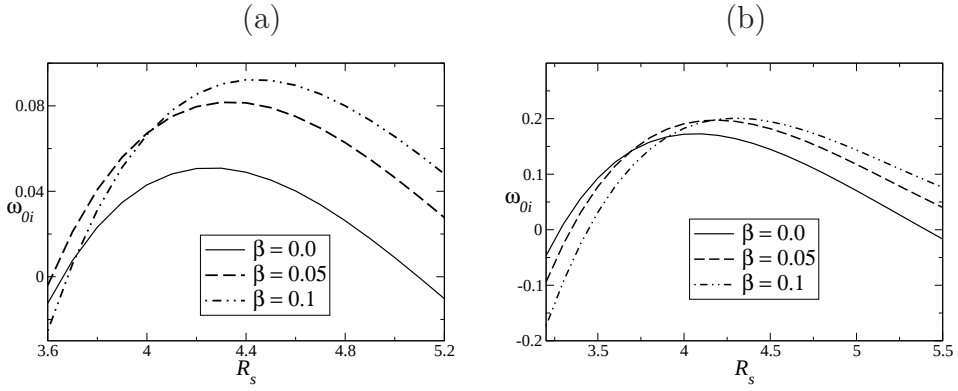

Figure 8: The slip effects on the absolute growth rate ω_{0i} (at the saddle point) as a function of log-mobility ratio (R_s) of slower diffusing species (S): (a) $q = 0.1$ and (b) $q = 0.05$. The other parameters are $Re = 200$, $R_f = -0.5$, $Sc = 50$, $h = 0.6$ and $\delta = 10$.

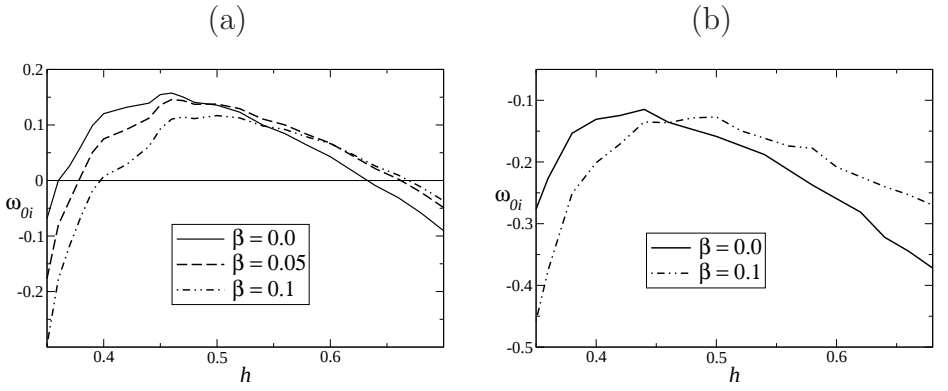

Figure 9: The slip effects on the absolute growth rate ω_{0i} (at the saddle point) as a function of the location of the mixed layer (h) for $Re = 200$, $q = 0.1$: (a) DD flow with $R_s = 4.0$, $R_f = -0.5$, $Sc = 50$, $\delta = 10$ and (b) SC(E) flow with $R_s = 3.5$, $R_f = 0.0$, $Sc = 9.09$, $\delta = 10$.

In order to understand the influence of the location of the mixed layer on the absolute instability growth rate ω_{0i}, the results are presented in Fig. 9(a) (DD flow with $Re = 200$, $R_s = 4.0$, $R_f = -0.5$, $Sc = 50$, $\delta = 10$ and $q = 0.1$) and in Fig. 9(b) (SC(E) flow with $Re = 200$, $R_s = 3.5$, $R_f = 0.0$, $Sc = 9.09$, $\delta = 10$ and $q = 0.1$). Note that ω_{0i} is highly influenced by

the location of the mixed layer (q). When the mixed layer is nearer the center line ($y = 0$), then the DD system is not absolutely unstable. As the mixed layer moves towards the wall ($h < 0.5$), ω_{0i} becomes positive and the DD flow system is absolutely unstable; but in a slippery channel, the absolute growth rate decreases with increase in β. The largest absolute growth rate for each β is seen around $h \cong 0.45$; that is, when the mixed layer overlaps the critical layer. **The critical layer is a thin layer around the critical point y_c (say) where, the base velocity is equal to the phase speed of the two dimensional disturbances i.e., $U_B(y_c) = c_r$.** As h increases further, the role of slip on absolute growth rate is nonmonotonic for the DD flow. Also, as the distance of the mixed layer from the channel wall is decreased, there is a decrease in the absolute growth rate and this decrease is more significant for the DD flows in a rigid channel than in a slippery channel. It is inferred from Fig. 9(b) that the equivalent SC(E) system is not absolutely unstable for any position of mixed layer when $Re = 200$ in both the rigid and the slippery channels.

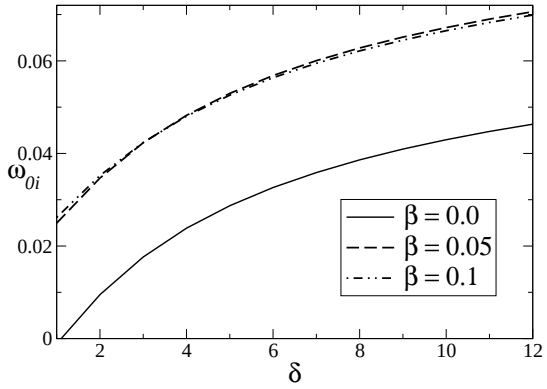

Figure 10: Effects of δ and β on the absolute growth rate ω_{0i} (at the saddle point) of the DD system for $Re = 200$, $R_s = 4.0$, $R_f = -0.5$, $Sc = 50$, $h = 0.6$ and $q = 0.1$.

As the ratio δ of diffusion rates of the two components increases, the absolute growth rate increases for each β, when the mixed layer is nearer the channel wall ($h = 0.6$, Fig. 10) with other parameters as $Re = 200$, $R_s =$

4.0, $R_f = -0.5$, $Sc = 50$ and $q = 0.1$. But at any δ, ω_{0i} is very significant for a slippery channel DD flow system. Although at smaller δ, larger wall slip has larger absolute growth rate and at higher δ, a reverse trend is seen, the differences are negligible. The absolute instability is stronger for a DD system ($\delta > 1$) than for an SC system ($\delta = 1$) both in rigid and slippery channel.

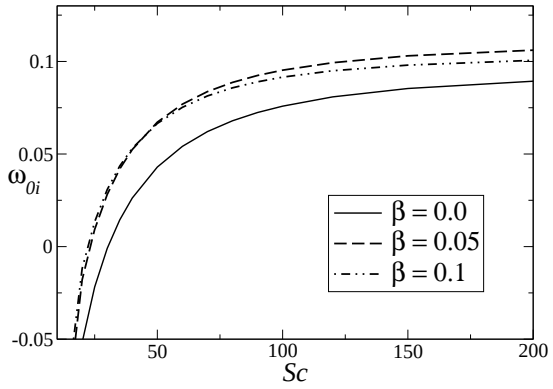

Figure 11: Absolute growth rate ω_{0i} (at the saddle point) as a function of diffusivity (Sc) for the DD system with different slip (β). All other parameters are taken as $Re = 200$, $R_s = 4.0$, $R_f = -0.5$, $\delta = 10$ and $q = 0.1$.

The effect of solutal diffusivity (Sc) on the absolute growth rate (ω_{0i}) is summarized in Fig. 11. The DD system in both the rigid and slippery channels are absolutely unstable beyond a certain Sc value. The DD system in a rigid channel ($\beta = 0.0$) is stabilized as is evident from the critical Sc value and the absolute growth rate. The results are presented for $Re = 200$, $R_s = 4.0$, $R_f = -0.5$, $\delta = 10$ and $q = 0.1$. While for smaller Sc ($Sc < 50$), destabilization effect of β is exhibited, there is a nonmonotonic behaviour with slip for $Sc > 50$. Further, a DD flow in a rigid channel is not absolutely unstable for some Sc values (say $Sc \simeq 28$), but that in a slippery channel, is absolutely unstable. In general, Sc has destabilizing effect on the DD system. However, for each β beyond a certain value of Sc, the instability is unaltered over a range of Schmidt number (Sc). For very small Sc, the system is convectively unstable ($\omega_{0i} < 0$) but not absolutely unstable.

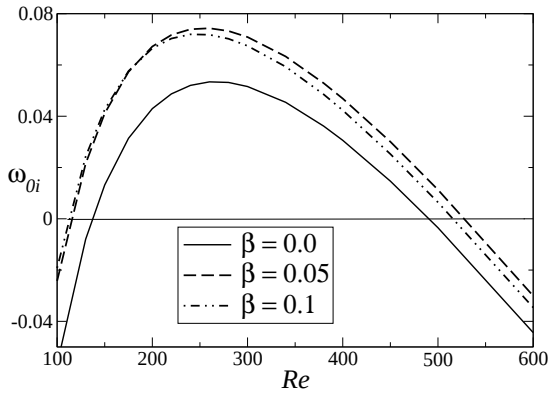

Figure 12: Influence of Reynolds number (Re) on the absolute instability for the DD system at different values of β. The other parameters are $R_s = 4.0$, $R_f = -0.5$, $Sc = 50$, $\delta = 10$ and $q = 0.1$.

The inertial forces also have an influence on the absolute instability of the DD flow is evident from Fig. 12 ($R_s = 4.0$, $R_f = -0.5$, $Sc = 50$, $\delta = 10$ and $q = 0.1$). At the onset of the absolute instability, slip has a destabilizing role by increasing the absolute growth rate (ω_{0i}) at the saddle point. Beyond the critical Re, where inertial forces are stronger than the viscous forces, the slip exhibits a nonmonotonic behaviour with respect to ω_{0i}. The range of Reynolds number for which absolute growth rate is positive, increases with increase in slip. There is a range of Reynolds number in which the DD flow in a rigid channel is only convectively unstable while the DD flow in a slippery channel is absolutely unstable.

4. Conclusions

The absolute and/or convective instability of the double-diffusive miscible two-fluid Poiseuille flow in a slippery channel is analyzed for a configuration with increasing viscosity towards the slippery channel walls. The viscosity has exponential dependence on the log-mobility ratios of two diffusing components/species (with different rate of diffusions). A Briggs type method is employed to examine the spatio-temporal instability.

For smaller values of log-mobility ratio of the slower diffusing species (R_s), the DD flow system with mixed layer closer to the slippery wall with highly viscous upper layer, in a rigid channel is absolutely unstable (Fig. 8(a), (b); solid lines for $\beta = 0$) but the same flow system in a slippery channel is stable (Fig. 8(a), (b); $\beta = 0.1$). A similar trend is also observed for higher values of R_s but for the mixed region placed close to the centre line (Fig. 9(a)). For certain parameter regimes where the DD flow system in a rigid channel is not absolutely unstable (Fig. 8(a), (b); solid lines for $\beta = 0$), become absolutely unstable in a slippery channel (Fig. 8(a), (b); solid lines for $\beta \neq 0$). The DD system with highly viscous fluid is absolutely unstable only for a range of Reynolds numbers, which increases with increasing the wall slip (Fig. 12).

For the DD systems wherein fluid viscosity decreases towards the walls, it is found that the Reynolds number at which instability (convective) sets in for slippery channel is lower than that of rigid channel. When the fluid viscosity increases towards the wall, the DD miscible two-fluid flows in rigid as well as slippery channels are both convectively and absolutely unstable. The growth rates are higher as compared to the corresponding SC systems. An interesting and striking observation in the present study is the enhanced absolute growth rate for the DD flow system in slippery channel.

The enhancement of absolute instability by wall slip in some parameter regimes (when the slower diffusing species is destabilizing) can be favourably used to achieve early transition to turbulence by designing the channel walls as hydrophobic surfaces or rough/porous surfaces with small permeability, as such surfaces can be modelled by wall-slip.

Appendix A: Justification for constant mixed layer thickness

The following discussion show how the parallel flow and the constant mixed layer thickness assumptions are justified for slow diffusion (higher value of Peclet numbers).

Let a splitter plate be located at $x < x_0$, at a constant y and let the parallel streams of two miscible fluids flow on both sides of this plate. The streams come into contact with each other at $x = x_0$. The two fluids begin to mix with each other for $x > x_0$, thus producing a stratified layer. The thickness 'q' of this layer grows as the fluids move downstream and therefore q is a function of x. In what follows, it is shown that the thickness of the mixed layer varies slowly in x, i.e $\partial q/\partial x \ll 1$.

We know at any location, the steady mean concentrations f and s corresponding to two spices F and S satisfy the equations,

$$U\frac{\partial f}{\partial x} + V\frac{\partial f}{\partial y} = \frac{\delta}{Pe}\left[\frac{\partial^2 f}{\partial x^2} + \frac{\partial^2 f}{\partial y^2}\right], \tag{A1}$$

$$U\frac{\partial s}{\partial x} + V\frac{\partial s}{\partial y} = \frac{1}{Pe}\left[\frac{\partial^2 s}{\partial x^2} + \frac{\partial^2 s}{\partial y^2}\right], \tag{A2}$$

respectively. Now under the boundary layer approximation ($V \ll U$ and $\frac{\partial^2}{\partial x^2} \ll \frac{\partial^2}{\partial y^2}$), we will get from Eq. (A1),

$$U\frac{\partial f}{\partial x} \simeq \frac{\delta}{Pe}\frac{\partial^2 f}{\partial y^2}. \tag{A3}$$

Also, using the same approximation, we know that $U \sim O(1)$, $y \sim \sqrt{\nu}$, where ν is the kinematic viscosity. Note that the viscosity is directly proportional to the concentration of each fluid in the mixed layer. Therefore, $qf \sim O(y^2)$ since f is the mean concentration over the mixed layer of thickness q. This implies that $\partial f/\partial x \simeq \frac{1}{q}O(\delta/Pe)$ (from Eq. (A3)). Similarly from Eq. (A2), we can get $\partial s/\partial x \simeq \frac{1}{q}O(1/Pe)$. So, for large values of Pe, $\partial f/\partial x$, $\partial s/\partial x$ are very small, showing that the downstream variation of f and s are very small which in turn implies that the changes in the thickness q of the mixed layer along the x-direction is very small.

Appendix B: Briggs type method for finding absolute and convective instabilities

The approach employed to distinguish the convective and absolute instabilities involves the association of a differential operator for the perturbations (namely ϕ, s and f) in physical space with the dispersion relation in complex (ω, α) space and the subsequent introduction of a Green's function $G(x, y, t)$, that represents the impulse response of the flow. The latter can be expressed as a double Fourier integral in the complex ω and α planes along contours C_ω and C_α respectively, [12, 37, 43, 44] which are chosen in order to satisfy causality considerations. Variation of ω along C_ω is associated with spatial branches in the complex α plane, α^+ and α^-, located in the upper and lower half planes, respectively. The contour C_α lies between α^+ and α^- in order to satisfy causality requirements.

In order to determine the stability characteristics, the behaviour of the function $G(x, y, t)$ at long times is determined along different "rays" corresponding to constant values of x/t. This can be done by first using the method of steepest descent [43, 52], which involves determining the saddle point of the exponent of G, α_*. The saddle point condition is

$$\frac{\partial \omega}{\partial \alpha}(\alpha_*) = \frac{x}{t}, \tag{A1}$$

which is real and corresponds to the group velocity. The contour C_α, originally coinciding with the α_r axis, is then deformed into the path of steepest descent through α_* so that the behaviour of $G(x, y, t)$ is dominated by the contribution of the region nearest to α_*,

$$G(x, y, t) \sim \frac{e^{\mathrm{i}[\pi/4 + \alpha_* x - \omega(\alpha_*)]}}{\frac{\partial D}{\partial \omega}[\alpha_*, \omega(\alpha_*)] \left[2\pi \frac{\partial^2 \omega}{\partial \alpha^2}\right]^{1/2}}, \tag{A2}$$

As can be seen from Eq. (A2), the temporal growth rate measured by an observer moving along a ray x/t is $\omega_{*,i} - (x/t)\alpha_*$. To determine whether the flow is linearly stable or unstable, one first finds the maximum temporal

growth rate, $\omega_{i,max} = \omega_i(\alpha_{max})$ where α_{max} is real and satisfies $\frac{\partial \omega_i}{\partial \alpha}(\alpha_{max}) = 0$. The flow is then said to be

(a) linearly stable if $\omega_{i,max} < 0$,

(b) linearly unstable if $\omega_{i,max} > 0$.

In order to determine whether the flow is convectively or absolutely unstable, one first determines the so-called "absolute frequency", $\omega_0 = \omega(\alpha_0)$, where α_0 the "absolute wavenumber", may be complex and satisfies

$$\frac{\partial \omega}{\partial \alpha}(\alpha_0) = 0. \tag{A3}$$

This corresponds to the ray $x/t = 0$ or zero group velocity. The "absolute growth rate", ω_{0i}, measures disturbance growth or decay along the ray $x/t = 0$ i.e., in a stationary reference frame. The flow is then said to be [43, 44, 48]

(a) absolutely unstable if $\omega_{0i} > 0$,

(b) convectively unstable if $\omega_{0i} < 0$.

Physically, if a localized disturbance generated by an impulse spreads both upstream and downstream from its source, the flow is absolutely unstable; if, on the other hand, the disturbance amplitude grows downstream of the source, the flow is convectively unstable.

The $x/t = 0$ condition given by Eq. (A3) coincides with the contour C_ω coming into contact with the locus of any temporal branches in the complex ω plane at ω_0; if this event is accompanied by C_ω being in the upper (lower) half planes then the flow is absolutely (convectively) unstable[12]. The zero group velocity condition also coincides with the pinching of the contour C_α when the branches α^+ and α^-, initially located in the upper and lower half planes[43, 44], respectively, come into contact at α_0. The presence of such singularities in both the complex α and ω plane are very important.

[1] S. Ghosh, R. Usha and K. C. Sahu, "Double-diffusive two-fluid flow in a slippery channel: A linear stability analysis," Phys. Fluids **26**, 015412 (2014).

[2] J.S. Turner, "Double-diffusive phenomena," Ann. Rev. Fluid Mech. **6**, 37-54 (1974).

[3] H. E. Huppert, "On the stability of a series of double-diffusive layers," Deep-Sea Res. Oceanogr. Abstr. **18**(10), 1005-1021 (1971).

[4] B. D. May and D. E. Kelley, "Effect of baroclinicity on double-diffusive interleaving," J. Phys. Oceanogr. **27**, 1997-2008 (1997).

[5] M. G. Worster "Time-dependent fluxes across double-diffusive interfaces," J. Fluid Mech. **505**, 287-307 (2004).

[6] S. Ghosh, R. Usha and K. C. Sahu, "Linear stability anlysis of miscble two-fluid flow in a channel with velocity slip at the walls," Phys. Fluids **26**, 014107 (2014).

[7] R. J. Deissler , "The convective nature of instability in plane Poiseuille flow," Phys. Fluids **30**, 2303 (1987).

[8] R. Valette, P. Laure, Y. Demay and J. Agassant, , "Convective linear stability analysis of two-layer coextrusion flow for molten polymers," J. Non-Newtonian Fluid Mech. **121**, 41-53 (2004).

[9] B. T. Ranganathan and R. Govindarajan, "Stabilisation and destabilisation of channel flow by location of viscosity-stratified fluid layer," Phys. Fluids. Lett. **13(1)**, 1 (2001).

[10] R. Govindarajan, "Effect of miscibility on the linear instability of two-fluid channel flow," Int. J. Multiphase Flow **30**, 1177 (2004).

[11] P. Ern, F. Charru, and P. Luchini, "Stability analysis of a shear flow with strongly stratified viscosity," J. Fluid Mech. **496**, 295 (2003).

[12] K. C. Sahu, P. Valluri, H. Ding and O. K. Matar, "Linear stability analysis and numerical simulation of miscible channel flow," Phys. Fluids **21**, 042104 (2009).

[13] K. C. Sahu, and O. K. Matar, "Three-dimensional linear instability in pressure-driven two-layer channel flow of a Newtonian and a Herschel-Bulkley fluid," Phys. Fluids **22**, 112103 (2010).

[14] K. C. Sahu and R. Govindarajan, "Linear stability of double-diffusive two-fluid channel flow," J. Fluid Mech. **687**, 529 (2011).

[15] K. C. Sahu and R. Govindarajan, "Spatio-temporal linear stability of double-diffusive two-fluid channel flow," Phys. Fluids **24**, 054103 (2012).

[16] R. Govindarajan and K. C. Sahu, "Instabilities in viscosity-stratified flows," Ann. Rev. Fluid Mech. **Vol. 46**, 331-353 (2014).

[17] E. H. Kennard, *Kinetic Theory of Gases* (McGraw-Hill, New York, 1938).

[18] G. A. Bird, *Molecular Gas Dynamics and the Direct Simulation of Gas Flows* (Oxford University Press, Great Clarendon Street, Oxford, 1994).

[19] D. C. Tretheway and C. D. Meinhart, "Apparent fluid slip at hydrophobic microchannel walls," Phys. Fluids **14**, L9 (2002).

[20] C. H. Choi, K. J. A. Westin, and K. S. Breur, "Apparent slip flows in hydrophilic and hydrophobic microchannels," Phys. Fluids **15**, 2897 (2003).

[21] J. Kim and C. J. Kim, "Nanostructured surfaces for dramatic reduction of flow resistance in droplet-based microfluidics," Technical Digest, IEEE conference on MEMS, Lasvegas, NV **ISSN 1084-6999**, p.479 (2002).

[22] M. M. Denn, "Extrusion instabilities and wall slip," Ann. Rev. Fluid Mech. **33**, 265 (2001).

[23] J. W. Hoyt, "Hydrodynamic Drag Reduction Due to Fish Slimes," Swimming and Flying, Nature **2**, 653 (1975).

[24] D. W. Bechert, M. Bruse, W. Hage, and R. Meyer, "Fluid Mechanics of Biological Surfaces and their Technological Applications," Naturwissenschaften **87**, 157 (2000).

[25] Y. Zhu and S. Granick, "Rate-dependent slip of Newtonian liquid at smooth surfaces," Phys. Rev. Lett. **87**, 096105 (2001).

[26] P. A. Thompson and S. M. Troian, "A general boundary condition for liquid flow at solid surfaces," Nature **389**, 360 (1997).

[27] J. M. Gersting, "Hydrodynamic stability of plane porous slip flow," Phys. Fluids **17**, 2126 (1974).

[28] A. Spille and H. B. A. Rauh, "Critical curves of plane Poiseuille flow with slip boundary conditions," Nonlinear Pheonomena in Complex Systems **3**, 171 (2000).

[29] C. J. Gan and Z. N. Wu, "Short-wave instability due to wall slip and numerical observation of wall-slip instability for microchannel flws," J. Fluid Mech. **550**, 289 (2006).

[30] E. Lauga and C. Cossu, "A note on the stability of slip channel flows," Phys. Fluids **17**, 088106 (2005).

[31] R. Ling, C. Jian-Guo, and Z. Ke-Qin, "Dual role of wall slip on linear stability of plane Poiseuille flow," Chin. Phye. Lett **25**, 601 (2008).

[32] K. C. Sahu, A. Sameen, and R. Govindarajan, "The relative roles of divergence and velocity slip in the stability of plane channel flow," Eur. Phys. J. Appl. Phys. **44**, 101 (2008).

[33] X. Y. You and J. R. Zheng, "Stability of liquid-liquid stratified microchannel flow under the effects of boundary slip," Int-J. Chemical Reactor Eng. **7**, A85 (2009).

[34] M. Webber, "Instability of fluid flows, including boundary slip," Doctoral thesis, Durham University - **Available at Durham E-Theses Online: http://etheses.dur.ac.uk/2308/**, (2007).

[35] T. Min and J. Kim, "Effects of hydrophobic surface on stability and transition," Phys. Fluids **17**, 108106 (2005).

[36] J. P. Pascal, "Linear stability of fluid flow down a porous inclined plane," J. Phys. D: Appl. Phys **32**, 417 (1999).

[37] K. C. Sahu, and O. K. Matar, "Three-dimensional convective and absolute instabilities in pressure-driven two-layer channel flow," Int. J. Multiphase Flow **37(8)**, 987-993 (2011).

[38] P. Neogi and C. A. Miller, "Spreading kinetics of a drop on a rough solid surface," J. Colloid Interface Sci. **92**, 338 (1983).

[39] A. Wierschem, M. Scholle, and N. Aksel, "Vortices in film flow over strongly undulated bottom profiles at low Reynolds numbers," Phys. Fluids **15**, 426-435 (2003).

[40] M. Scholle, A. Wierschem, and N. Aksel, "Creeping films with vortices over strongly undulated bottoms," Acta. Mech. **168**, 167-193 (2004).

[41] A. Wierschem and N. Aksel, "Influence of inertia on eddies created in films creeping over strongly undulated substrates ," Phys. Fluids **16**, 4566-4574 (2004).

[42] A. Rund, M. Scholle, and N. Aksel, "Drag reduction and improvement of material transport in creeping films," Arch. Appl. Mech. **75**, 93-112 (2006).

[43] P. Huerre and P. A. Monkewitz, "Local and global instabilities in spatially developing flows," Ann. Rev. Fluid Mech. **22**, 473-537 (1990).

[44] R. J. Briggs, *Research Monograph No.* **29**, (MIT Press, Cambridge, 1964)

[45] P. G. Drazin and W. H. Reid, *Hydrodynamic stability* (Cambridge University Press, Cambridge, 1985).

[46] C. Canuto, M. Y. Hussaini, A. Quarteroni, and T. A. Zang, *Spectral Methods in Fluid Dynamics*, 1st edn. ed. (Springer Verlag, New York, 1987).

[47] J.-M. Chomaz, "Global instabilities in spatially developing flows: Non-normality and nonlinearity," Ann. Rev. Fluid Mech. **37**, 357 (2005).

[48] A. Bers, inHandbook of Plasma Physics, edited by M. N. Rosenbluth and R. Z. Sagdeev (North-Holland, Amsterdam, 1983), **Vol. 1**, pp. 451517.

[49] I. Vihinen, A. M. Honohan, and S. P. Lin, "Image of absolute instability in a liquid jet," Phys. Fluids **9(11)**, 3117 (1997).

[50] W. O. Criminale, T. L. Jackson and R. D. Joslin, *Theory and computation of hydrodynamic stability* (Cambridge University Press, New York, 2003).

[51] L. Kaiktsis and P. A. Monkewitz, "Global destabilization of flow over a backward-facing step," Phys. Fluids **15(12)**, 3647(2003).

[52] C. M. Bender and S. A. Orszag, *Advanced Mathematical Methods for Scientists and Engineers: Asymptotic Methods and Perturbation Theory* (McGraw-Hill, New York, 1978).